Fabrication of flat SiGe heterostructure nanomembrane windows via strain-relief patterning

2015 J. Phys. D: Appl. Phys. 48 015306

(http://iopscience.iop.org/0022-3727/48/1/015306)

IOP Publishing Journal of Physics D: Applied Physics
J. Phys. D: Appl. Phys. **48** (2015) 015306 (6pp) doi:10.1088/0022-3727/48/1/015306

Fabrication of flat SiGe heterostructure nanomembrane windows via strain-relief patterning

K M McElhinny[1], G Gopalakrishnan[1,4], D E Savage[1], Juan C Silva-Martínez[1,2], M G Lagally[1], M V Holt[3] and P G Evans[1]

[1] University of Wisconsin-Madison, Madison, WI 53706, USA
[2] Department of Chemical Engineering, University of Puerto Rico-Mayaguez, Mayaguez, Puerto Rico 00681, USA
[3] Center for Nanoscale Materials, Argonne National Laboratory, Argonne, IL 60439, USA

E-mail: evans@engr.wisc.edu

Received 29 August 2014, revised 21 October 2014
Accepted for publication 3 November 2014
Published 3 December 2014

Abstract
The lattice mismatch between SiGe and Si in heteroepitaxial Si/SiGe/Si trilayers leads to buckling when confined nanomembrane windows formed from these heterostructures are released from silicon-on-insulator substrates. We demonstrate that large areas in which the curvature and curvature-induced strain are reduced by an order of magnitude can be produced by patterning the windows to concentrate buckling in narrow arms with low flexural rigidity supporting a flat central region. Synchrotron x-ray thermal diffuse scattering shows that the improved flatness of patterned windows permits fundamental studies with fidelity similar to what can be achieved with flat single-component Si nanomembranes.

Keywords: nanomembrane, strain, buckling, silicon, silicon–germanium

(Some figures may appear in colour only in the online journal)

1. Introduction

Silicon–germanium (SiGe) nanostructures provide the opportunity to control electronic and thermal properties via nanoscale engineering while working within the versatile Si materials platform. With respect to thermoelectric technologies, for example, SiGe quantum wells and superlattices exhibit reduced thermal conductivity [1–4], which forms the basis for devices with improved thermoelectric figures of merit [5–7]. Extremely thin crystals, in the form of released windows or sheets, combine the functionality and versatility afforded by nanoscale dimensions with the excellent crystal quality and precise control of composition available via epitaxial growth [8, 9]. SiGe epitaxial heterostructure membranes have been fabricated in geometries that include completely released and transferred nanosheets [10], and rolls in which curvature is driven by the lattice mismatch between Si and SiGe [8, 9]. The creation of very flat Si/SiGe membrane windows, however, has proven to be extremely challenging because a combination of the Si/SiGe epitaxial mismatch and residual stress arising from membrane fabrication can lead to buckling when the elastic boundary condition provided by the growth substrate is released. The challenge is to create flat Si/SiGe nanomembranes that are separated from a silicon-on-insulator (SOI) substrate over large areas but which are still mechanically supported by the substrate. Meeting this challenge requires confining the buckling of the Si/SiGe heterostructure to isolated areas in order to minimize the curvature and curvature-induced strain in a spatially separate flat region. We demonstrate that large flat regions of supported Si/SiGe/Si trilayer nanomembranes can be produced by patterning the Si/SiGe/Si windows to create regions of low flexural rigidity before their release from the substrate and that such windows have sufficient flatness to permit scattering studies of their fundamental properties.

[4] Author to whom any correspondence should be addressed.
Present address: University of Wisconsin-Platteville, Platteville, WI 53818, USA

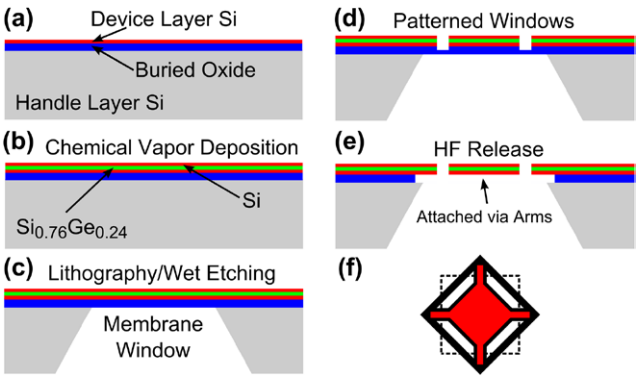

Figure 1. Fabrication of Si/SiGe/Si trilayer nanomembranes. (*a*) Starting SOI. (*b*) Deposition of the $Si_{0.76}Ge_{0.24}$ and Si layers by CVD. (*c*) Fabrication of membrane windows via photolithography and anisotropic etching in KOH. (*d*) Creation of strain-relief pattern by photolithography and reactive ion etching. (*e*) Release of membrane from BOX layer in HF. (*f*) Plan view of the strain-relief pattern. Dashed lines indicate the edges of the membrane window opened in step (*c*).

2. Experimental

The process shown in figure 1 can be used to create structures with sufficient mechanical compliance to yield Si/Si0.74Ge0.26/Si trilayer membranes with minimum mechanical distortion. The SOI starting material had a 400 nm-thick buried oxide (BOX) layer (figure 1(*a*)) and a 100 nm-thick device layer that was subsequently thinned to 20 nm via wet thermal oxidation and hydrofluoric acid (HF) etching. Epitaxial SiGe and top Si layers were grown on the SOI device layer using chemical vapor deposition (CVD) (figure 1(*b*)). A 200 nm-thick non-stoichiometric low-stress silicon nitride (SiN_x) layer was grown on all surfaces of the sample by low-pressure CVD at 850 °C to serve as a protective coating and as a patternable etch mask. The back of the handle wafer was patterned by photolithography and reactive ion etching (RIE) of the SiN_x. Windows consisting of BOX, Si/SiGe/Si, and SiN_x were created by removing the handle wafer in the exposed areas using an anisotropic etch in KOH. The SiN_x layer was then removed in hot phosphoric acid (figure 1(*c*)).

To release the constraint imposed by the edges, narrow arms supporting a large central region were patterned into the SiGe membranes before the final removal of the BOX. The arms were created using optical lithography and RIE to remove the trilayer in selected areas, leaving a pattern of 20 μm-wide arms connected to a central 100 × 100 μm square area (figure 1(*d*)). The trilayer membrane was then released and undercut in concentrated HF, as shown in figure 1(*e*). A plan-view schematic diagram of the arm pattern is shown in figure 1(*f*). The pattern is oriented so that the edges of the square membrane are at an angle of 45 ° with respect to the edges of the window in the handle wafer. Four strain relieving arms are aligned along the Si <1 1 0> directions, and the edges of the supported central region are parallel to <1 0 0> . An alternative arrangement of the supporting arms is based on a large number of narrower strain relieving bars [11, 12]. This alternative allows strain to be relieved by in-plane deflection with independent control over the in-plane and out-of-plane stiffness and often includes a buckling of the supporting arms in the plane of the membrane [11, 12]. The single narrow arm structure was selected here, however, in order to eliminate the possibility that instabilities in the etching and drying of the multiple bar structure would complicate their fabrication, including the adhering of several bars together resulting in fracture.

3. Results and discussion

In an unconstrained Si/SiGe/Si heteroepitaxial membrane the mismatch in lattice constant between SiGe and Si produces biaxial compression of the SiGe layer and biaxial expansion in the Si layers [13]. Epitaxial growth of a Si/SiGe/Si trilayer on a rigid Si substrate, however, results in the compression of the SiGe layer with respect to its equilibrium lattice constant before release, which leads to an overall biaxial expansion after release. The fabrication of flat membrane windows from stressed layers is challenging because windows are fixed to the original substrate at their edges, and thus cannot relax by expanding laterally, making the flat configuration of the membrane unstable with respect to buckling out of the plane of the surface [14, 15].

Buckling occurs due to a minimization of the elastic energy by an out-of-plane distortion of the initially planar structure. The elastic energy is reduced by buckling when the lateral extent of the window is larger than the critical length of the buckling instability. This critical buckling length can be approximated using $l_c \approx \pi h\sqrt{\frac{1}{3\varepsilon}}$, where ε is the residual compressive strain and h is the thickness of the membrane [11]. The study presented here employs $Si/Si_{0.74}Ge_{0.26}/Si$ trilayer membranes with a total thickness of 60 nm and an average compressive strain of 0.3% before release. The critical buckling length for these structures is less than 2 μm, which would yield windows that are impractically small for many fundamental studies and applications of released membranes.

Insight into the processes through which flattened SiGe membranes can be created is obtained by considering the strategies that are used to create flat large-area Si nanomembranes. Si membrane windows are compositionally identical to the surrounding materials, but can be distorted after release because residual stress is imparted into the Si nanomembranes during the thinning or release processes [8, 9, 11, 12, 16–18]. The magnitude of the residual stress is sufficient to lead to lateral expansion of approximately 0.1% when the Si membranes are released [19]. Flat Si membrane windows can be created from SOI by mechanically accommodating the expansion caused by the residual stress [19, 20]. Among the strategies through which the buckling can be removed from Si membrane windows is edge-induced flattening, in which an undercut region in the BOX extends past the edges of the Si membrane window, resulting in the Si membrane being flattened due to interfacial forces during drying [19]. The maximum excess length that can be removed by edge-induced flattening is approximately twice the thickness of the BOX layer.

The edge-induced flattening methods applicable to Si membranes are ineffective in creating flat Si/SiGe/Si trilayer

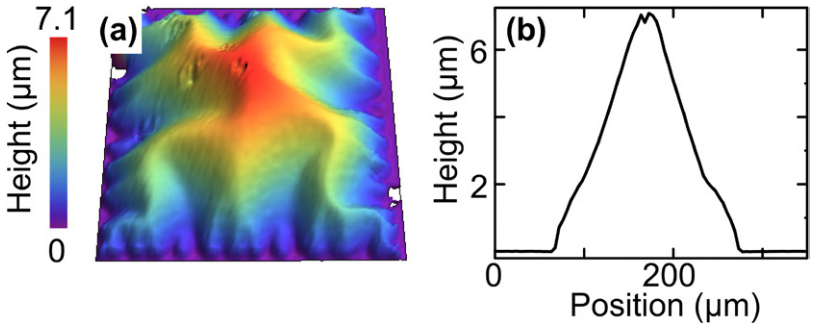

Figure 2. (*a*) White-light interferometry height map of a buckled 60 nm-thick Si/$Si_{0.76}Ge_{0.24}$/Si trilayer window. The lateral extent of the released window is 200 μm. (*b*) Height profile along a line through the center of membrane, parallel to the bottom edge of the map.

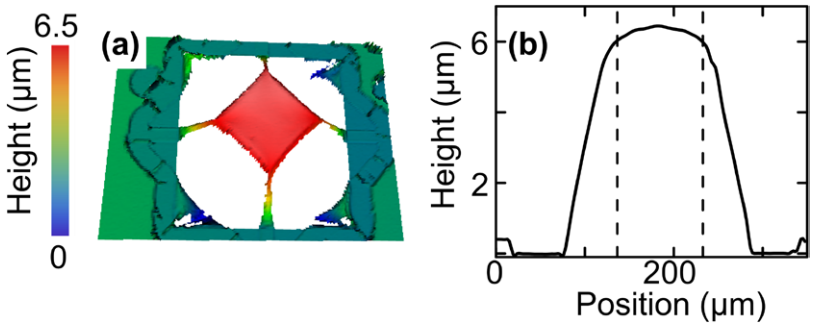

Figure 3. (*a*) White-light interferometry height map of the strain-relief patterned 60 nm-thick trilayer. (*b*) Height of the patterned trilayer membrane along a line passing horizontally through the center of the membrane and along two of the arms connecting the central region of the membrane to the substrate. Dashed vertical lines indicate the locations of the ends of the supporting arms.

membranes because (i) the thicknesses of the silicon layers of the membrane are not perfectly matched during epitaxy, which can lead to a preferred direction of curvature in the released membrane, and (ii) the lattice constant reached by force equilibrium between the Si and SiGe layers is significantly larger than that of unstrained Si. The large strain in the Si/SiGe system requires a flattening strategy based on a structure that can accommodate a larger maximum in-plane expansion than is available through edge-induced flattening. Engineered support structures have previously been used to flatten single-layer membranes with micron-scale thicknesses and lateral extents of tens to hundreds of μm [11, 12, 16].

The buckling resulting from the release of a 200 × 200 μm edge-supported square Si/SiGe/Si membrane window is apparent in the white-light interferometry height map shown in figure 2(*a*). The maximum vertical displacement along a horizontal line through the center of the membrane window is 7.1 μm, as in figure 2(*b*). The central region of the unpatterned Si/SiGe/Si membrane has a radius of curvature of 235 μm. With the simplifying approximation that the buckling completely relieves the elastic stress, the excess length of the buckled membrane in figure 2(*b*) corresponds to a compressive strain before release of 0.35%. The strain arising from the force balance between the Si and SiGe layers in a linear elastic model for a completely relaxed membrane with the same thickness and composition is 0.29% [13]. The excellent agreement between the experimentally observed magnitude of the released strain and the contribution from the Si/SiGe mismatch leads us to conclude that the strain in the Si/SiGe/Si trilayer before release arises from the Si/SiGe lattice mismatch. Residual strain in the device layer of the parent SOI would also lead to buckling, as it does in Si membranes fabricated from SOI [19]. We suspect, however, that in this case the residual stress in the SOI is small compared to stress from the lattice mismatch, and that it has a minimal contribution to the buckling instability in Si/SiGe/Si trilayers.

A map of the vertical displacements in a strain-relieved Si/SiGe/Si membrane is shown in figure 3(*a*). Regions of high curvature are confined to 10 μm-wide regions near the both ends of each supporting arm, as shown in the plot of the vertical height as a function of position in figure 3(*b*). The curvature where the supporting arms connect to the substrate is five times greater than the curvature where the supporting arms connect to the central region of the membrane. This concentration of the curvature at the substrate end of the arms occurs as a result of the greater rigidity of the substrate compared to the membrane. The radius of curvature across the central region of the membrane supported by narrow arms is 2350 μm. In comparison, the radius of curvature of the same region of the unpatterned membrane is 235 μm. Hence, the introduction of the narrow arms results in an increase of the radius of curvature by a factor of 10, and a corresponding decrease in the curvature-induced strain and strain gradient.

The confinement of the curvature to the arms is consistent with the expectation that the larger flexural rigidity of the central region, arising from its comparatively large area, forces the curvature to be concentrated in the arms to reduce the total elastic energy. In the dimension x along the length of an

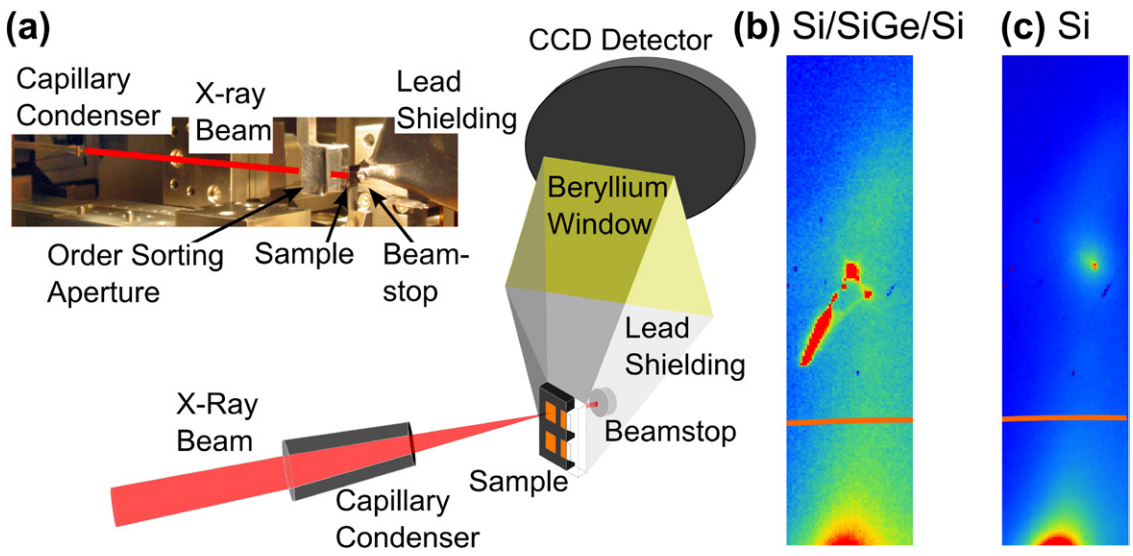

Figure 4. (*a*) Experimental arrangement for x-ray thermal diffuse scattering measurements. The x-ray beam is focused to a 30 μm spot size by a capillary condenser. The focused beam passes through an order-sorting aperture before illuminating the sample in a transmission geometry. The direct beam is stopped by a lead beamstop and the scattered x-rays are collected by a CCD detector. X-ray diffuse scattering patterns acquired from (*b*) a strain-relief patterned 60 nm-thick trilayer membrane, and (*c*) a 21 nm-thick flat silicon membrane flattened using the procedure described in [19]. The sharp intense features near the center of the TDS intensity distribution in (*b*) are an artifact arising from powder x-ray diffraction from material outside the membrane illuminated by a small fraction of the incident beam.

arm the elastic strain energy per unit length due to bending is $\frac{1}{2}D\frac{w(x)}{R(x)^2}$ [21]. Here $w(x)$ and $R_c(x)$ are the width and radius of curvature, respectively, as a function of the position x along the structure. The flexural rigidity per unit width is given by $D = \frac{Eh^3}{12(1-\nu^2)}$, where E is Young's modulus and ν is Poisson's ratio. Fabricating structures in which $w(x)$ is locally reduced allows the total elastic energy to be minimized by decreasing the radius of curvature in the narrow regions. The further localization of the curvature to the ends of the narrow arms is consistent with the expectation that the arm/membrane geometry closely approximates a clamped-guided beam, which in turn can be approximated as two back-to-back end-loaded beams [22]. In elastic calculations for a geometry corresponding to figure 3, the curvature is concentrated over approximately 1/3 of the length of the arm [21].

The flatness of membranes supported by narrow arms permits more sophisticated fundamental studies to be performed with them than would be possible with buckled windows. In order to evaluate the suitability of the flattened membranes for studies of their vibrational properties, synchrotron x-ray thermal diffuse scattering (TDS) measurements were performed at station 26-ID of the Advanced Photon Source at Argonne National Laboratory using an experimental arrangement previously described [19, 23]. Incident x-rays with a photon energy of 10 keV were focused to a spot size of 30 μm on the center of the membrane using a capillary condenser x-ray optic. The membrane was oriented in a transmission geometry in which scattered x-rays were collected by a charge-coupled device (CCD) detector, as shown in figure 4(*a*). The experiment was performed in vacuum and employed extensive shielding to minimize contributions to the detected intensity caused by scattering from beamline optical components.

Figures 4(*b*) and (*c*) show the TDS signals from a 60 nm-thick $Si/Si_{0.76}Ge_{0.24}/Si$ trilayer and a 21 nm-thick Si membrane, respectively. The 60 nm-thick $Si/Si_{0.76}Ge_{0.24}/Si$ trilayer was flattened by the strain-relief patterning described here while the 21 nm-thick Si membrane was flattened by edge-induced flattening, which has previously been shown to produce membranes of sufficient flatness for use in TDS studies [19, 23, 24]. The orientations of the membrane surfaces and crystallographic axes with respect to the incident beam and detector are nearly identical for both samples. The truncation rod of the $13\bar{1}$ reflection of the membrane lattice produces an intense sharp feature at the right side of the scattering patterns of both samples. The orange line overlaid on the detector image represents the intersection of the Ewald sphere with the zone boundary between the first Brillouin zones of the $13\bar{1}$ and 220 reflections.

Bright features at the bottoms of the images in figures 4(*b*) and (*c*) are the TDS from near the center of the neighboring zone centered on the 220 reflection. The diffuse streak of intensity extending upwards through the center of the image towards a second area of higher intensity is TDS resulting from high populations in the lower-frequency phonon modes along the high-symmetry <1 1 1> directions in Si and SiGe. The TDS from the Si/SiGe/Si trilayer can be resolved with clarity similar to the TDS from the silicon nanomembrane, which would not be possible if the Si/SiGe/Si trilayer nanomembrane was buckled as in figure 1(*a*). The saturated streak of intensity in the Si/SiGe/Si scattering pattern in figure 4(*b*) arises from x-ray diffraction from material outside the membrane illuminated by a small fraction of the incident beam that was not completely suppressed by the shielding of the detector. Diffuse scattering studies of distorted membranes yield a broad featureless background overwhelming the intensity due to TDS [19].

4. Conclusion

The strain relief patterning procedure described here allows large flat membranes to be produced in heterostructures that would otherwise exhibit prohibitively large buckling distortions. The buckling is localized at the end of strain-relief arms, creating flat membranes in which the curvature and strain are reduced by an order of magnitude relative to NMs without strain relief arms. The flattened membranes resulting from this process provide model systems for fundamental scientific studies of crystalline sheets with nanoscale thicknesses, free from the influence of a supporting substrate and with greatly reduced artifacts from strain variations and curvature. In addition, within the SiGe/Si nanomembrane system flattened structures can find applications in freestanding chemical and gas sensors [25, 26], micro- and nano-electro-mechanical devices [27–29], thermal waveguides and thermal diodes [30], and flexible thin film transistors with high-current drive capacity and high electron mobility [10].

Acknowledgments

GG, KM, and PE acknowledge support from the US Air Force Office of Scientific Research, through contract FA9550-10-1-0249. Trilayer growth (DES and MGL) was supported by the US Department of Energy, grant number DE-FG02-03ER46028. Nanomembranes were fabricated at the Wisconsin Center for Applied Microelectronics at the University of Wisconsin-Madison supported in part by the UW MRSEC (NSF DMR-1121288), and at the Center for Nanoscale Materials at Argonne National Laboratory. The Center for Nanoscale Materials is a U.S. Department of Energy, Office of Science, Office of Basic Energy Sciences user facility supported by contract No. DE-AC02-06CH11357. Use of the Advanced Photon Source was supported by the U. S. Department of Energy, Office of Science, Office of Basic Energy Sciences, under Contract No. DE-AC02-06CH1135.

References

[1] Singh D, Murthy J Y and Fisher T S 2011 Effect of phonon dispersion on thermal conduction across Si/Ge interfaces *J. Heat Transfer* **133** 122401

[2] Huxtable S T, Abramson A R, Tien C-L, Majumdar A, LaBounty C, Fan X, Zeng G, Bowers J E, Shakouri A and Croke E T 2002 Thermal conductivity of Si/SiGe and SiGe/SiGe superlattices *Appl. Phys. Lett.* **80** 1737

[3] Liu C-K, Yu C-K, Chien H-C, Kuo S-L, Hsu C-Y, Dai M-J, Luo G-L, Huang S-C and Huang M-J 2008 Thermal conductivity of Si/SiGe superlattice films *J. Appl. Phys.* **104** 114301

[4] Lee S-M, Cahill D G and Venkatasubramanian R 1997 Thermal conductivity of Si–Ge superlattices *Appl. Phys. Lett.* **70** 2957

[5] Yang B, Liu W L, Liu J L, Wang K L and Chen G 2002 Measurements of anisotropic thermoelectric properties in superlattices *Appl. Phys. Lett.* **81** 3588–90

[6] Koga T, Cronin S B, Dresselhaus M S, Liu J L and Wang K L 2000 Experimental proof-of-principle investigation of enhanced Z3DT in (0 0 1) oriented Si/Ge superlattices *Appl. Phys. Lett.* **77** 1490

[7] Tripathi M N and Bhandari C M 2007 Thermal and thermoelectric behavior of silicon–germanium quantum well structures *Eur. Phys. J. B–Condens. Matter* **59** 503–8

[8] Rogers J A, Lagally M G and Nuzzo R G 2011 Synthesis, assembly and applications of semiconductor nanomembranes *Nature* **477** 45–53

[9] Scott S A and Lagally M G 2007 Elastically strain-sharing nanomembranes: flexible and transferable strained silicon and silicon–germanium alloys *J. Phys. Appl. Phys.* **40** R75

[10] Yuan H-C, Wang G, Ma Z, Roberts M M, Savage D E and Lagally M G 2007 Flexible thin-film transistors on biaxial- and uniaxial-strained Si and SiGe membranes *Semicond. Sci. Technol.* **22** S72

[11] Iwase E, Hui P-C, Woolf D, Rodriguez A W, Johnson S G, Capasso F and Lončar M 2012 Control of buckling in large micromembranes using engineered support structures *J. Micromech. Microeng.* **22** 065028

[12] Hijab R S and Muller R S 1989 Residual strain effects on large aspect ratio micro-diaphragms *IEEE Micro Electro Mechanical Systems, 1989, Proc., An Investigation of Micro Structures, Sensors, Actuators, Machines and Robots* (*Salt Lake City, UT*) pp 133–8

[13] Mooney P M, Cohen G M, Chu J O and Murray C E 2004 Elastic strain relaxation in free-standing SiGe/Si structures *Appl. Phys. Lett.* **84** 1093–5

[14] Ziebart V, Paul O, Munch U, Schwizer J and Baltes H 1998 Mechanical properties of thin films from the load deflection of long clamped plates *J. Microelectromech. Syst.* **7** 320–8

[15] Ziebart V, Paul O and Baltes H 1999 Strongly buckled square micromachined membranes *J. Microelectromech. Syst.* **8** 423–32

[16] Graff J and Schubert E 2000 Flat free-standing silicon diaphragms using silicon-on-insulator wafers *Sensor Actuators Phys.* **84** 276–9

[17] Lee K C 1990 The fabrication of thin, freestanding, single-crystal, semiconductor membranes *J. Electrochem. Soc.* **137** 2556–74

[18] Torres C M S, Zwick A, Poinsotte F, Groenen J, Prunnila M, Ahopelto J, Mlayah A and Paillard V 2004 Observations of confined acoustic phonons in silicon membranes *Phys. Status Solidi C* **1** 2609–12

[19] Gopalakrishnan G, Czaplewski D A, McElhinny K M, Holt M V, Silva-Martínez J C and Evans P G 2013 Edge-induced flattening in the fabrication of ultrathin freestanding crystalline silicon sheets *Appl. Phys. Lett.* **102** 033113

[20] Shchepetov A, Prunnila M, Alzina F, Schneider L, Cuffe J, Jiang H, Kauppinen E I, Sotomayor Torres C M and Ahopelto J 2013 Ultra-thin free-standing single crystalline silicon membranes with strain control *Appl. Phys. Lett.* **102** 192108

[21] Landau L D and Lifshitz E M 1986 *Theory of Elasticity* (New York: Pergamon)

[22] Legtenberg R, Groeneveld A W and Elwenspoek M 1996 Comb-drive actuators for large displacements *J. Micromech. Microeng.* **6** 320

[23] Gopalakrishnan G, Holt M V, McElhinny K M, Spalenka J W, Czaplewski D A, Schülli T U and Evans P G 2013 Thermal diffuse scattering as a probe of large-wave-vector phonons in silicon nanostructures *Phys. Rev. Lett.* **110** 205503

[24] Gopalakrishnan G, Holt M V, McElhinny K M, Czaplewski D A and Evans P G 2013 Probing large wavevector phonons at the nanoscale via x-ray thermal diffuse scattering *Adv. X-Ray Anal.* **56** 82

[25] Houlet L F, Shin W, Nishibori M, Izu N, Itoh T and Matsubara I 2008 Fabrication and performance of free-standing hydrogen gas sensors *Sensor Actuators B Chem.* **129** 1–9

[26] Yu M, Huang M, Savage D E, Lagally M G and Blick R H 2011 Local-wetting-induced deformation of rolled-up Si/Si-Ge nanomembranes: a potential route for remote chemical sensing *IEEE Trans. Nanotechnol.* **10** 21–5

[27] Schmidt O G, Deneke C, Manz Y M and Müller C 2002 Semiconductor tubes, rods and rings of nanometer and micrometer dimension *Phys. E Low-Dimens. Syst. Nanostruct.* **13** 969–73

[28] Schmidt O G, Deneke C, Schmarje N, Muller C and Jin-Phillipp N Y 2002 Free-standing semiconductor micro- and nano-objects *Mater. Sci. Eng. C-Biomim. Supramol. Syst.* **19** 393–6

[29] Prinz V Y, Seleznev V A, Prinz A V and Kopylov A V 2009 3D heterostructures and systems for novel MEMS/NEMS *Sci. Technol. Adv. Mater.* **10** 034502

[30] Maldovan M 2013 Narrow low-frequency spectrum and heat management by thermocrystals *Phys. Rev. Lett.* **110** 025902